Progress In Electromagnetics Research Letters, Vol. 75, 19–24, 2018

Quasi-Millimeter Wave Technique Used for Image of Wood

Dan Zhang[1, *], Chujing Zong[1], and Atsushi Mase[2]

Abstract—A quasi-millimeter electromagnetic wave with the frequency of 22–30 GHz is applied to detect knots and holes in wood samples. It has better spatial resolution while keeping good transmission properties comparied to microwave region used in the previous experiments. The images of knots and holes in wood are clearly obtained by analyzing the phase and amplitude of the transmitted wave. And the phase measurement results are all better than amplitude results according to phase values changing much more than amplitude.

1. INTRODUCTION

Several approaches have been explored for knot and defect detection in wood using the microwave range of electromagnetic waves [1–5]. However, efforts for knot detection by microwaves have not achieved a sufficient level suitable for industrial applications. The quasi-millimeter-wave technique has an electromagnetic frequency range from 22 to 30 GHz, which offers higher spatial resolution than the microwave technique and higher transmission properties than millimeter or terahertz waves which are also used for the nondestructive evaluation of wood [6–11]. However the millimeter-wave technique can be used to measure the transmitted amplitude of only 2 mm thick wood slices [8, 9]. To the best of our knowledge, few people have used this quasi-millimeter band 22–30 GHz to detect wood. In addition, the frequency and the bandwidth are assigned by the Administration of Radio under the Ministry of Internal Affairs and Communications. Quasi-millimeter wave with this frequency band is one of the candidates that the outdoor use is permitted when its output power is low. The purpose of this study was to obtain good imaging of the knots and holes in wood through quasi-millimeter wave. This paper presents the design and construction of a simple transmission system that permits detection of holes or knots in fir wood boards or white poplar cut logs at a laboratory.

2. MEASUREMENT SYSTEM AND FORMULA

The electrical field propagation through a loss medium can be calculated according to electromagnetic theory as follows:

$$\mathbf{E}(z,t) = \left(\mathbf{E}_0 e^{-\alpha z}\right) e^{-j\beta z} \cdot e^{j\omega t} \tag{1}$$

For electromagnetic wave propagation in medium, the increase of the electromagnetic wave with z will have energy dissipation. $\gamma = \alpha + j\beta$ is the propagation constant, α the attenuation constant, and β the phase constant of the electromagnetic field. For low moisture content, the expressions for α and β can be simplified from the binomial expansion of Eq. (1):

$$\alpha = \omega \left[\frac{\mu\varepsilon}{2}\left(\sqrt{1+\tfrac{\sigma^2}{\omega^2\varepsilon^2}}-1\right)\right]^{\frac{1}{2}} = \omega\sqrt{\frac{\mu\varepsilon}{2}}\left[\left\{1+\frac{1}{2}(\tan\delta)^2\right\}-1\right]^{\frac{1}{2}} \cong \frac{1}{2}\omega\sqrt{\mu\varepsilon}\tan\delta \tag{2}$$

Received 19 February 2018, Accepted 28 March 2018, Scheduled 9 April 2018
* Corresponding author: Dan Zhang (zhangdan@njfu.edu.cn).
[1] College of Information Science and Technology, Nanjing Forestry University, Nanjing 210037, China. [2] Global Innovation Center, Kyushu University, Kasuga, Fukuoka 816-8580, Japan.

$$\beta = \omega\left[\frac{\mu\varepsilon}{2}\left(\sqrt{1+\frac{\sigma^2}{\omega^2\varepsilon^2}}+1\right)\right]^{\frac{1}{2}} = \omega\sqrt{\frac{\mu\varepsilon}{2}}\left[\left\{1+\frac{1}{2}(\tan\delta)^2\right\}+1\right]^{\frac{1}{2}} \cong \omega\sqrt{\mu\varepsilon}\left[1+\frac{1}{8}(\tan\delta)^2\right] \cong \omega\sqrt{\mu\varepsilon} \quad (3)$$

Figure 1 shows the schematic of the quasi millimeter wave measurement system. For transmission measurement, a vector network analyzer (VNA) is utilized. The P1 port of the VNA is connected to an incident cable. The transmitted wave is detected by a P2 port of the VNA. A Ka band horn antenna (1 mW) connected with the VNA is used as a transmitter and placed the distance to the wood sample obverse surface as 6 cm in order to produce a uniform plane wave which can vertically incidence the surface, and also passes through the sample to a waveguide tube used as a receiver which distance to sample reverse surface is 1 cm. A display and a portable computer connected to the VNA will show the S parameters and allow data processing. The amplitude of transmitted wave measured is expressed as $20\log E_t$, and the phase shift ϕ expressed as $\phi = \beta z$.

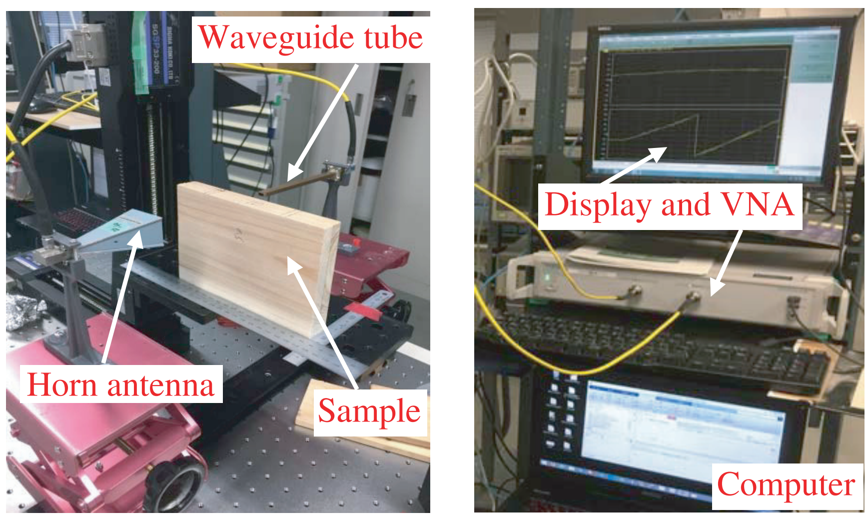

(a)

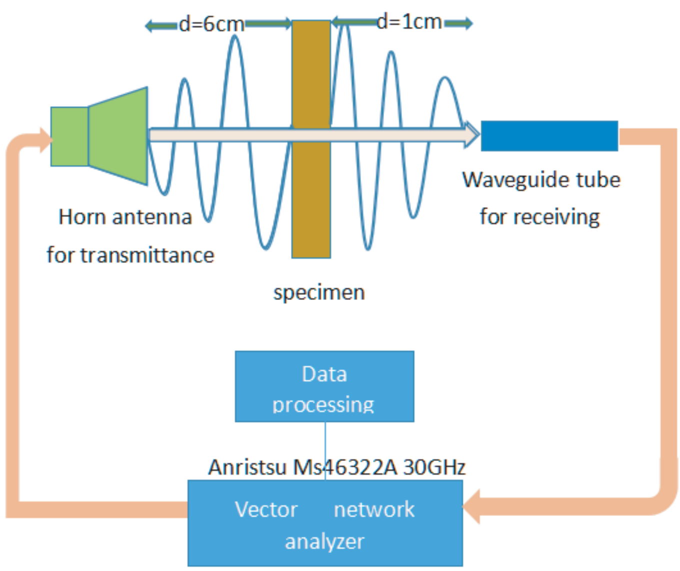

(b)

Figure 1. Experimental set-up for the quasi millimeter wave measurement system. (a) The photo of the measurement system. (b) The measurement schematic diagram.

The output is modulated by a chirped wave with a modulation sensitivity of $\Delta\omega/\Delta t$

$$\omega = \omega_0 + (\Delta\omega/\Delta t)\, t \quad \gamma = \gamma_0 + (\Delta\gamma/\Delta t)\, t \tag{4}$$

The transmitted wave through wood is given by

$$\mathbf{E}_t \propto \mathbf{E}_0 e^{-\gamma \Delta z} e^{j\omega t} \tag{5}$$

The displacement of the propagation constant during frequency modulation is calculated as

$$\Delta\Gamma = (\Delta\gamma/\Delta t) \cdot (\Delta z/c) = \left(\frac{\Delta\omega}{c} \cdot \sqrt{\varepsilon}\right)\left(\frac{1}{2}\tan\delta + j\right)\Delta z \tag{6}$$

The displacement of phase is shown as

$$\Delta\Phi = \left(\frac{\Delta\omega}{c} \cdot \sqrt{\varepsilon}\right)\Delta z \tag{7}$$

The real part of the dielectric constant and loss tangent in air dry wood are $\varepsilon_r \sim 4$ and $\tan\delta \sim 0.1$, MC = 12% respectively. Since the modulation frequency is $\Delta\omega = 30\text{–}22\,\text{GHz} = 8\,\text{GHz}$, the amplitude of transmitted wave becomes $E_t = 0.95E_i$ when passing through a 2 cm thick wood. E_i is the amplitude of incidence wave. If the values changed by a factor of 2 depending on the passage position, the amplitude would only change to $E_t = 0.90E_i$. However, the corresponding phase values would change by as much as 50 to 80 degrees. Therefore, the phase measurement can distinguish differences in transmission.

3. EXPERIMENTAL RESULTS

We used a fir wood ($\rho = 0.376\,\text{g/cm}^3$) board without knots and holes as the control, as shown in Fig. 2.

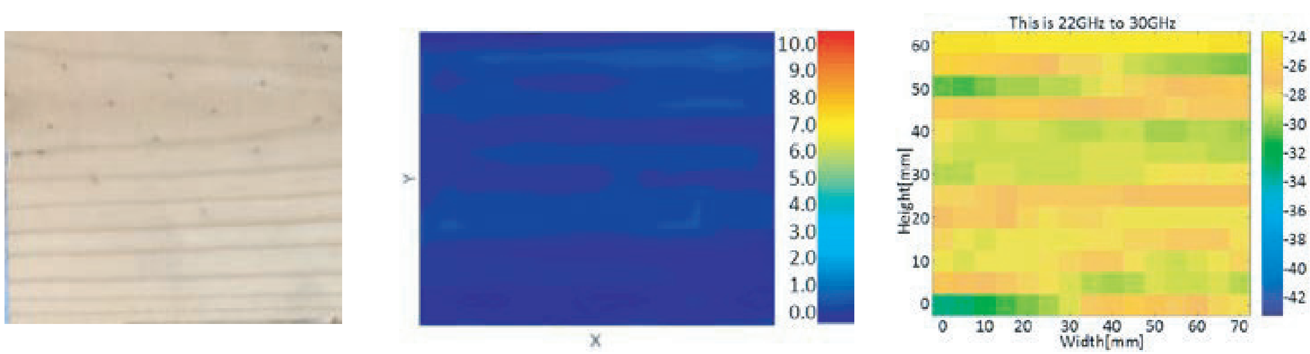

(a) (b) (c)

Figure 2. (a) Image of a 2 cm thick fir wood board without knots. (b) The phase diagram of the sample shown in (a). (c) The amplitude diagram of the sample shown in (a).

In the resulting image, there are no holes and knots, and the amplitude image color contrast is very small. For the wood board with holes or knots, the color contrast will be more obvious. Another sample of 2 cm thick fir wood board with knots is shown in Fig. 3. The changes of phase and amplitude in the transmitted wave are applied to observe the internal profile of woods. As shown in Fig. 3, there is a marked change in the color of the area of knot, with a difference between them of about 10 in the phase measurement. In the amplitude measurement, there is also a color contrast; however, the difference is not so clear as the phase measurement.

The third sample is 6 cm thick cut white poplar log ($\rho = 0.380\,\text{g/cm}^3$) with a drilled side hole 13 mm in diameter, as shown in Fig. 4. The color contrast distribution is obvious for this sample. The phase values of the hole and core area (suspected knot) in the blue region are approximately -10, the values of the hole and core part edge in the yellow region are approximately -3, and orange is a normal portion of the sample with a phase value of 0. From the phase diagram of the sample, we can see that the left blue area corresponds to the side hole, the big blue area in the middle corresponds to the knot which

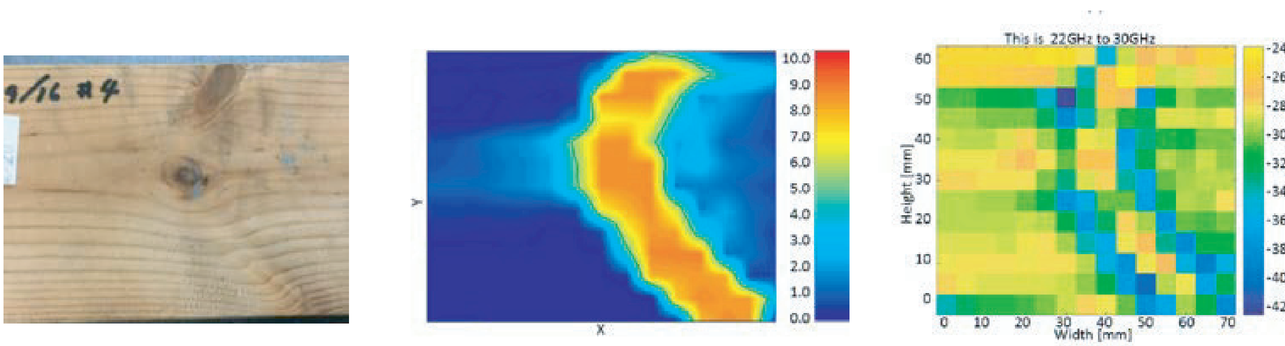

(a) (b) (c)

Figure 3. (a) Image of a 2 cm thick fir wood board with knots. (b) The phase diagram of the sample shown in (a). (c) The amplitude diagram of the sample shown in (a).

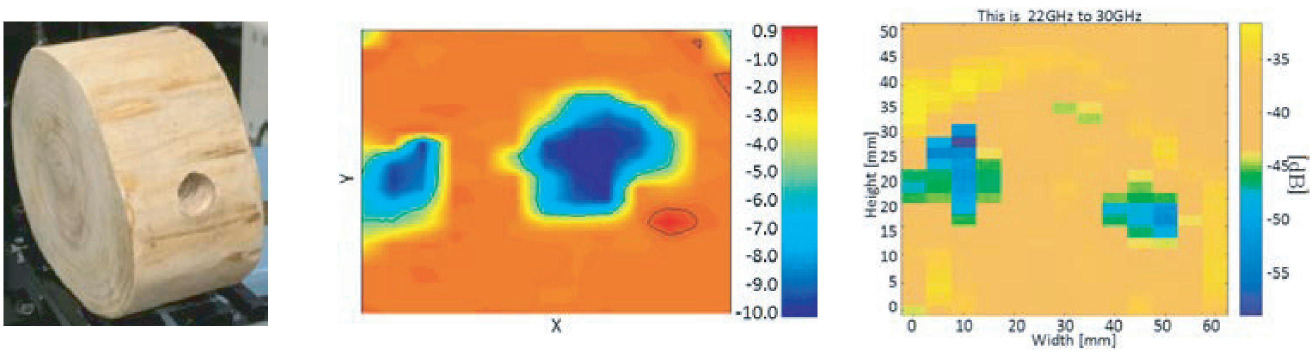

(a) (b) (c)

Figure 4. (a) Image of a 6 cm thick white poplar log with a side hole diameter of 13 mm. (b) The phase diagram of the sample shown in (a). (c) The amplitude diagram of the sample shown in (a).

we cannot find inside the wood with naked eye. In the amplitude diagram, the left side corresponds to the side hole, the right corresponds to the amplitude of the edge of the knot. The difference between the hole or knot and the normal wood is great, because the permittivity of the knot or hole is larger or smaller than the normal wood. The observed change in amplitude is consistent with the phase change. We can find that the phase detection is more sensitive than amplitude one.

The fourth sample is also a 6 cm thick cut white poplar log with sharp knots, as shown in Fig. 5. In the phase diagram, the dark blue area are knots, the light blue area are the edge of the knots. The blue region of -7 values corresponds to the knot, and there is clear contrast with the normal portion of the wood. We can also see some circle areas, because there are some contrast with wooden wheels. In the amplitude diagram, the blue area also shows the loss due to the knots of the sample.

Finally, a 6 cm thick cut white poplar log sample is drilled with three different sized holes which diameters are 20 mm, 10 mm and 6 mm respectively. As shown in Fig. 6, we can find the amplitude values (-65 dB) is very low in the two small holes and the big hole edge areas (inside area of big hole is -30 dB). It means the waves can hardly pass through the two small holes and edge according to the electromagnetic edge effect and the holes work as a circular waveguides, the cut-off wavelength is $\lambda_c = 3.41$ radius. Therefore, the low frequency region of incident waves cannot propagate in the small size of holes. In the phase figure, the yellow circle on the right of 2.5 indicates the big hole inside portion, the blue region of -4.0 indicates the two small holes and the big hole edge. The value of the normal wood is about 6. In the amplitude diagram, the two blue circles on the left correspond to the two small holes, and the yellow circle near the middle corresponds to the big one. As shown in all results above, we can find that the phase measurement results are all better than amplitude results. Overall, this transmission system can be used to obtain the image, revealing the presence of knots or holes by the clear color contrast.

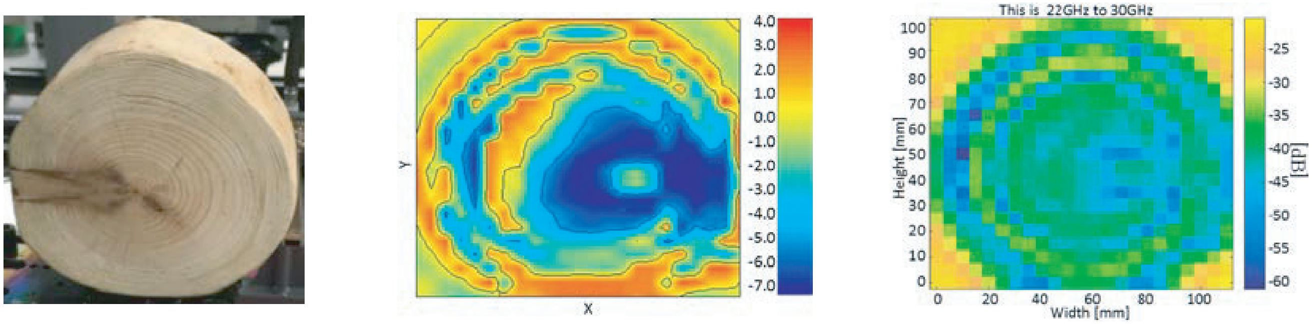

(a) (b) (c)

Figure 5. (a) Image of a white poplar wood log with sharp knots. (b) The phase diagram of the sample shown in (a). (c) The amplitude diagram of the sample shown in (a)

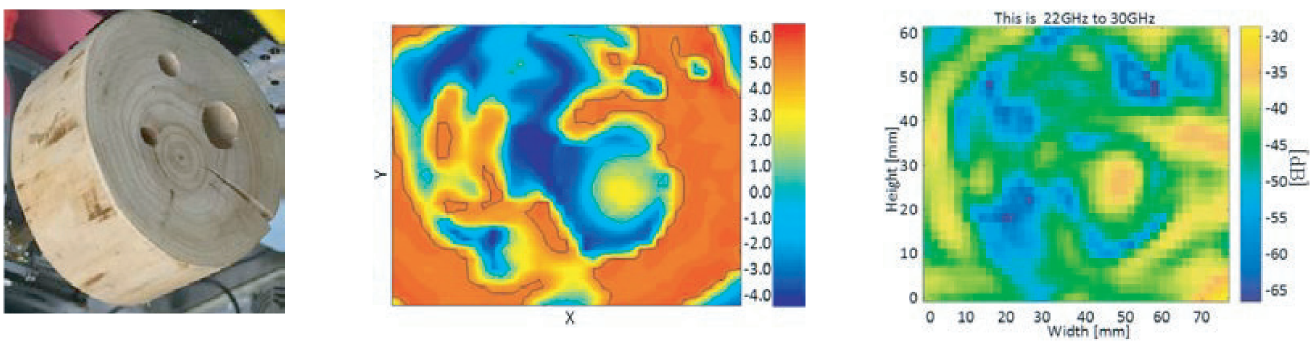

(a) (b) (c)

Figure 6. (a) Image of a white poplar log with drilled three different sizes holes. (b) The phase diagram of the white poplar sample shown in (a). (c) The amplitude diagram of the white poplar sample shown in (a)

4. CONCLUSION

In this work, we demonstrate that the proposed method reveals the existence of knots or holes, and can obtain good images. The phase measurement results are all better than amplitude results. In the knot-free-area, the color contrast is slight compared with other areas with knot. Many wood samples contain knots or holes inside that cannot be observed with the naked eye, but use of this quasi-millimeter wave technology allows detection.

REFERENCES

1. Hansson, L., N. Lundgren, A. L. Antti, and O. Hagman, "Microwave penetration in wood using imaging sensor," *Meas.*, Vol. 38, 15, 2005.
2. Johansson, J., O. Hagman, and B. A. Fjellner, "Predicting moisture content and density distribution of Scots pine by microwave scanning of sawn timber," *Wood Sci.*, Vol. 49, 312, 2003.
3. Bucur, V., *Nondestructive Characterization and Imaging of Wood*, 1, Springer, Berlin, 2003.
4. Schajar, G. S. and F. B. Orhan, "Microwave non-destructive testing of wood and similar orthotropic materials," *Subsurf Sens. Technol. Appl.*, Vol. 6, 293, 2005.
5. Fujii, Y., Y. Fujiwara, Y. Yanase, T. Mori, T. Yoshimura, M. Nakajima, H. Tsusumi, M. Mori, and H. Kurisaki, "Development of radar apparatus for scanning of wooden-wall to evaluate inner structure and bio-degradation non-destructively," *Adv. Mater. Res.*, Vol. 778, 289, 2013.
6. Baradit, E., R. Aedo, and J. Correa, "Knot detection in wood using microwaves," *Wood Sci. Technol.*, Vol. 40, 118, 2006.

7. Goldsmith, P. F., C. T. Hsieh, G. R. Huguenin, J. Kapitzky, and E. L. Moore, "Focal plane imaging systems for millimeter-wavelengths," *IEEE Trans. Microw. Theory. Tech.*, Vol. 41, 1644, 1993.
8. Tanaka, S., Y. Fujiwara, Y. Fujii, S. Okumura, H. Togo, N. Kukutsuand, and S. Mochizuki, "Effect of annual rings on transmission of 100 GHz millimeter waves through wood," *J. Wood Sci.*, Vol. 59, 375, 2013.
9. Tanaka, S., Y. Fujiwara, Y. Fujii, S. Okumura, H. Togo, N. Kukutsu, and T. Nagatsuma, "Effect of grain direction on transmittance of 100-GHz millimeter wave for hinoki (Chamaecyparis obtusa)," *J. Wood Sci.*, Vol. 57, 189, 2011.
10. Oyama, Y., L. Zhen, T. Tanabe, and M. Kagaya, "Sub-terahertz imaging of defects in building blocks," *NDT&E Int.*, Vol. 42, 28, 2009.
11. Wilcox, W. W., "Review of literature on the effects of early stages of decay on wood strength," *Wood Fiber*, Vol. 9, 252, 1978.